Deformation Behavior of Weakly Segregated Block Copolymers. 2. Correlation between Phase Behavior and Deformation Mechanisms of Diblock Copolymers

R. Weidisch,*,† G. Schreyeck,† M. Ensslen,‡ G. H. Michler,‡ M. Stamm,§ D. W. Schubert,|| H. Budde,⊥ S. Höring,⊥ M. Arnold,⊥ and R. Jerome#

Max-Planck-Institut für Polymerforschung, Postfach 3148, 55021 Mainz, Germany; Martin-Luther-Universität Halle-Wittenberg, Institut für Werkstoffwissenschaft, 06099 Halle, Germany; Institut für Polymerforschung Dresden e.V., Hohe Strasse 6, 01069 Dresden, Germany; GKSS Forschungszentrum, Max-Planck-Strasse, 21502 Geesthacht, Germany; Martin-Luther-Universität Halle-Wittenberg, Institut für Technische und Makromolekulare Chemie, 06099 Halle/Saale, Germany; and Center for Education and Research on Macromolecules, University of Liège, Sart Tilman B6, B-4000 Liège, Belgium

Received September 29, 1999

ABSTRACT: The deformation behavior of poly(styrene-*b*-butyl methacrylate) diblock copolymers, PS-*b*-PBMA, is studied by high-voltage electron microscopy (HVEM) with an in-situ tensile device. While in the first part the phase behavior of PS-*b*-PBMA diblock copolymers is investigated via small-angle neutron scattering (SANS), in the second part the deformation behavior depending on composition and molecular weight is discussed. Disordered block copolymers have the same deformation mechanism as the corresponding homopolymers, while microphase-separated block copolymers undergo a cavitation mechanism. At the order−disorder transition, ODT, a transition from crazing to cavitation mechanism is found via HVEM. Moreover, a sharp increase of the diameter of craze fibrils occurs at the ODT, demonstrating that the craze microstructure is strongly influenced by phase behavior. As the incompatibility increases with increasing molecular weight, deformation mechanisms such as diversion and termination of crazes are observed for intermediately segregated block copolymers. The discussed correlation between phase behavior and deformation mechanisms indicates the existence of a unified scheme for deformation behavior of diblock copolymers depending on the strength of segregation, χN.

Introduction

Block copolymers are nanometer-structuralized polymeric materials where the components show only a microphase separation. A larger variety of morphologies can be found in block copolymers compared to polymer blends. Therefore, different block copolymer systems were investigated with respect to their morphology and phase behavior in many studies. In poly(styrene-*b*-isoprene) (PS-*b*-PI) diblock copolymers bcc spheres, hexagonally packed cylinders and lamellar structures[1−3] were found. In the weak segregation limit the perforated layers and the cubic bicontinuous structure ("gyroid") were observed in addition.[4−6] The structures that can be found on the nanometer scale in block copolymers are interesting for different applications. For example, the high degree of transparency of block copolymers enables applications as packing materials. In most cases, mechanical properties are very important for industrial applications and require an optimum of stiffness, strength, and toughness. Of course, knowledge of different morphologies in block copolymers gives rise to the possibility of controlling the mechanical properties. However, control of the mechanical properties of block copolymers stems from knowledge of the parameters influencing the deformation behavior of different morphological types. Many studies examined the correlation between deformation behavior and morphology of PS−PB block copolymers.[7,8] Schwier et al.[9] proposed a model for craze growth in PS-*b*-PB diblock copolymers based on a mechanism of cavitation in the PB domains under the concentrated stresses of the craze tip. This is followed by drawing and fibril formation in the PS phase. It was shown that block copolymers do not show a crazing mechanism, because the microphase-separated morphologies on the nanometer scale are too small to initiate crazes.[10]

The deformation mechanism in block copolymers is much different from PS, where the craze growth occurs via the crazing mechanism. In PS, a local stress field builds up which is followed by the formation of crazes consisting of thin craze fibrils. The undeformed PS material will be transformed into craze fibril material (highly deformed PS) via the drawing mechanism. In contrast to crazing in PS, in block copolymers the first step of deformation is always[9] the deformation of the rubber phase up to a critical stress. This is followed by the formation of voids. The second step is the deformation of the glassy matrix and growth of crazes which is typically called a cavitation mechanism. The growth of crazes occurs by different mechanisms in PS (crazing) and diblock copolymers (cavitation).

The basic ingredients of the cavitation process are given in the tensile behavior of an idealized cube of material with ordered domains (spheres or hexagonally

† Max-Planck-Institut für Polymerforschung.
‡ Martin-Luther-Universität Halle-Wittenberg, Institut für Werkstoffwissenschaft.
§ Institut für Polymerforschung Dresden e.V.
|| GKSS Forschungszentrum.
⊥ Martin-Luther-Universität Halle-Wittenberg, Institut für Technische und Makro-molekulare Chemie.
University of Liège.
* Present address of corresponding author: Polymer Science and Engineering Department, University of Massachusetts, Amherst, MA 01003. E-mail: roland@squeaky.pse.umass.edu.

10.1021/ma991660v CCC: $19.00
Published on Web 06/29/2000

packed cylinder) in a glassy matrix. The sample is initially linearly elastic deformed up to a critical strain, where the rubbery domains cavitate under the local stresses. The stress builds up in the matrix and leads to a large plastic deformation of the glassy matrix with formation of fibrils directed by the local stress field. The investigation of Argon and co-workers showed[11] that a cavitation mechanism can be observed for different morphologies in PS-*b*-PB diblock copolymers. This is in agreement with our previous study attributed to the influence of morphology on the deformation of PS-*b*-PBMA diblock copolymers.[12]

Polis and Winey observed kink band formation in poly(styrene-*b*-ethylene propylene) diblock copolymers by applying steady shear strain.[13] Furthermore, the deformation behavior of PS-*b*-PB-*b*-PS triblock copolymers, SBS, at higher strains has been intensively investigated by TEM, SAXS, and SANS.[14−17] Recently, Thomas and co-workers[18] reported the deformation of gyroid phase in block copolymers. In our previous study, mechanisms of diversion and termination of crazes in PS-*b*-PBMA diblock copolymers were discussed which arise from the grain structure of the unoriented morphology.[12]

Understanding of the parameters that influence the deformation behavior of block copolymers will only obtained through more detailed studies. The most recent studies were focused on the influence of morphology on deformation behavior of block copolymers. In contrast, the present study focuses on the correlation between phase behavior and deformation mechanisms. The deformation behavior of block copolymers with varying strength of segregation should prove interesting to investigate. The study will focus on two sample series, with varying composition and molecular weight. An important question is whether the same deformation behavior can be observed for both disordered and ordered block copolymers; also, this would give a more deeper insight into the influence of microphase separation on deformation behavior. In the present study, we investigate PS-*b*-PBMA diblock copolymers, since this system shows a small interaction parameter between the components PS and PBMA. This allows comparison of different segregation states at higher molecular weights where the deformation structure and mechanical properties of the PS block do not show a molecular weight dependence. For the investigation of the correlation between phase behavior and deformation mechanism, it is necessary to begin with the discussion on the phase behavior of PS-*b*-PBMA diblock copolymers already investigated by Russell and co-workers.[19] Recently, Ruzette et al.[20] have shown that PS-*b*-alkyl methacrylate diblock copolymers with long side chain methacrylates ($n \geq 6$) reveal an upper critical order transition (UCOT) behavior. In contrast, diblock copolymers with short side chain methacrylates ($n < 5$) reveal a lower critical order transition (LCOT) behavior in the accessible temperature regime. In our previous study[21−23] we reported the morphologies and phase of PS-*b*-PBMA. In the present study, the composition dependence of interaction parameter, based on SANS experiments, will be discussed.

Experimental Section

Sample Preparation. All samples for deformation studies were dissolved in toluene. The solvent was allowed to evaporate slowly over 5−7 days at room temperature. Then the films were dried to constant weight in a vacuum oven at 120 °C for 3 days.

Table 1. Molecular Weight (M_n) and Volume Fraction (Φ_{PS}) for DPS-*b*-PBMA Diblock Copolymers (PS Block Deuterated) Used for SANS[a]

sample	$10^{-3}M_n$[b] copolymer	φ_{PS} block[c]	sample	$10^{-3}M_n$[b] copolymer	φ_{PS} block[c]
Molecular Weight Dependence					
1	69.000	0.47	5	121.000	0.51
2	90.000	0.55	6	151.000	0.50
4	105.000	0.43			
Composition Dependence					
7	121.000	0.16	13	91.000	0.48
8	95.700	0.21	14	90.000	0.55
9	99.000	0.30	15	125.000	0.64
10	132.000	0.36	16	136.000	0.76
11	112.000	0.37	17	135.000	0.84
12	100.700	0.38			

[a] Only these samples were used for calculation of χ where the inverse scattering intensity is linearly proportional to the invers temperature. [b] Total molecular weight and polydispersity determined by size exclusion chromatography (SEC). Values are based on the PS standards. The polydispersity of all samples is less than 1.1. [c] Volume fraction of PS as determined by ^{1}H NMR.

Characterization. The synthesis of PS-*b*-PBMA diblock copolymers was previously described by Arnold et al.[24] Measurements with size exclusion chromatography (SEC) were carried out using a Knauer-SEC with a RI/Viscodetector and a PS standard linear column. The volume fractions of the diblock copolymers were estimated by ^{1}H NMR. The molecular weights, compositions, and morphologies of diblock copolymers used in this study are summarized in Tables 1 and 2.

For the investigation of phase behavior, partially deuterated samples were used; i.e., the PS block of the copolymers was fully deuterated. Deuterated samples are denoted as dPS-*b*-PBMA. We assume that the deuteration has only a small influence on phase behavior. Small-angle neutron scattering (SANS) measurements were performed at the small-angle scattering facility SANS II located at GKSS Geesthacht (Germany). All used samples were melt-pressed into 1 mm thick and 13 mm diameter disks. The instrument configuration was as follows: a wavelength λ of 0.91 nm, a $\Delta\lambda/\lambda$ of 0.2 due to the velocity selector, and sample-to-detector distance of 5.6 m. The scattering data were corrected for detector sensitivity, background scattering, sample thickness, and sample transmission. The data were scaled to absolute units using several standards. The SANS profiles at different temperatures are discussed as a function of the scattering vector $q = (4\pi/\lambda)\sin(\theta)/2$, where θ is the scattering angle.

To investigate the micromechanical deformation behavior, sections with a thickness on the order of 0.5 μm were strained in a 1000 kV high-voltage electron microscope (HVEM, JEOL 1000) with an in-situ tensile device. This gives the possibility to study the craze growth and propagation. The advantage of HVEM investigations is the possibility to use thicker sections for closer comparison with bulk materials. Furthermore, external strained samples were investigated in the HVEM which allowed us to look at a possible decomposition of PBMA in the electron beam.

All investigations were performed at room temperature; however, a small increase of temperature during in-situ testing occurs arising from the electron beam. This effect can be partially avoided using externally strained samples. The strain rate as well as total strain can be controlled qualitatively during in-situ testing. However, the external strained samples provide more exact data concerning strain rate and total strain which can be controlled by a light microscope. The strain rate of all investigated samples is about 0.1 mm/min, and this may vary in different regions of the sample. All externally strained samples were deformed up to a strain near the yield point of about 2%, while the onset of crazing can be found at strains below the yielding point. Afterward, the external strained samples were investigated in the HVEM. The local strain is

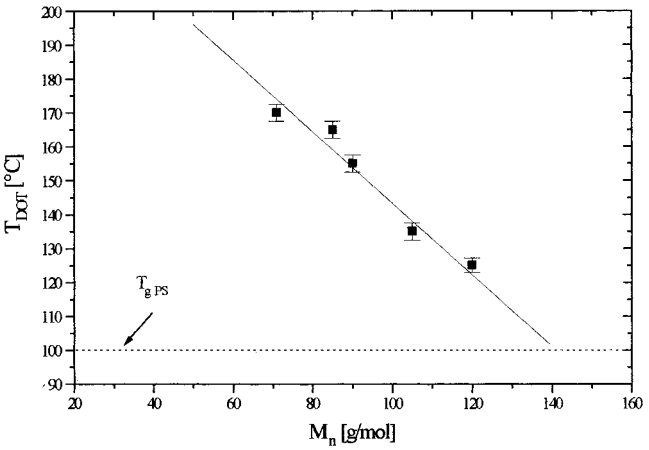

Figure 1. Dependence of disorder−order transition temperature, T_{DOT}, on molecular weight for PS-*b*-PBMA diblock copolymers (LCOT system) in Table 1 as observed by SANS and rheology.

usually much higher than the external strain which was found in PS and other polymers.[12,30] To get a more controlled craze growth, a small notch was introduced in all samples. The crazes propagate perpendicular to the direction of the stress applied in almost all cases. Only for the intermediately segregated sample SBM315 is the direction of external stress indicated in Figures 15 and 16.

Experimental Results and Discussion

1. Phase Behavior of Poly(styrene-*b*-butyl methacrylate) Diblock Copolymers. It was shown by Russell and co-workers[19] and in our previous studies[21] that PS-*b*-PBMA diblock copolymers show a LCOT depending on molecular weight. Samples with 70 kg/mol are disordered, yet for higher molecular weight samples the phases are microphase separated at all temperatures. It is shown in Figure 1 how the LCOT depends on molecular weight for dPS-*b*-PBMA diblock copolymers with about 50% dPS (Table 1).

The disorder−order temperature, T_{DOT}, increases with increasing molecular weight and shows a linear dependence on molecular weight. For a sample with molecular weight of 85 kg/mol, data from Russell et al.[19,20] are used to confirm the linear dependence. For molecular weights lower than 70 kg/mol a decomposition of the samples occurs above 180 °C, and a reversibility of the behavior is not found. The T_{DOT} approximates the T_g of the PS block with molecular weights about 130 kg/mol, so that the reversibility of the LCOT is also not achieved for high molecular weights. At higher molecular weights (M_n > 130 kg/mol) the diblock copolymers are microphase separated at all measured temperatures. Small differences exist in the T_{DOT} at different molecular weights between the study of Russell and co-workers[19,20] and our study due to small differences in composition of samples. We can conclude from our experiments that only a narrow range of molecular weights exists where the LCOT can be observed. This result agrees with our previous DMA and TEM experiments, where a lamellar structure was found for a sample with 130 kg/mol and 47% PS at temperatures higher than 100 °C.

As previously reported, PS-*b*-PBMA diblock copolymers show spherical, hexagonal, lamellar, gyroid, and perforated lamellar structures at higher molecular weights.[22,23,25] Figure 2 summarizes the morphologies of PS-*b*-PBMA diblock copolymers depending on molecular weight and composition as observed by TEM.[21−23,25] Recently, it was discussed that perforated lamellar and gyroid structures were not observed at the PS-rich side of the phase diagram. This could be attributed to the very high molecular weights used; an equilibrium is difficult to achieve.[23] In the composition range 72−76% PS a coexistence of lamellar and hexagonal structures is observed which is clearly not an equilibrium structure. It is shown in Figure 2 that samples with about 100 kg/mol are ordered only in the composition range $0.37 < \varphi_{PS} < 0.57$, whereas samples with other compositions are disordered. Block copolymers with molecular weights M_n > 120 kg/mol and about 70% PS show a lamellar structure.[22,23,25] A detailed discussion of the morphologies with respect to the phase boundaries is given in a recent paper.[25]

For a detailed discussion of the correlation between phase behavior and deformation mechanisms of PS-*b*-PBMA diblock copolymers, it is necessary to use the χN values of each sample. In our previous paper, the phase behavior of a dPS-*b*-PBMA diblock copolymer with 90 kg/mol and 50% dPS was discussed. From Leibler fits to neutron scattering profiles in the disordered state, it was possible to obtained the temperature dependence of the Flory−Huggins parameter.[21] In addtion, it is necessary to investigate asymmetrical compositions in the present study. Figure 3 shows two representative neutron scattering profiles, as well as the Leibler fits for block copolymers with different compositions. The agreement between the Leibler fit and the scattering curves is good over the entire scattering vector range. The experimental points at very small q ($q < 0.01$ nm^{-1}) are slightly larger than the fit. This disagreement could be due to the finite compressibility of the copolymer melt and polydispersity of the samples which is not taken into account in the theory. The temperature dependence of χ can be described as a sum of terms of entropic and enthalpic contributions, χ_S and χ_H. From the calculated scattering profiles, the temperature dependencies of χ are obtained for different compositions as shown in Figure 4a. For all samples, χ increases with increasing temperatures, indicating a LCOT behavior. The temperature dependence of χ is quite small compared to other block copolymers. It is obvious from Figure 4a that the entropic contribution to χ is relatively large compared to the enthalpic contribution. For PS-*b*-PMMA and PS-*b*-alkyl methacrylate diblock copolymers with long side chain methacrylates ($n \geq 6$), the entropic and enthalpic contributions are comparable in size with our system. However, these systems show an UCOT behavior.[20,26] It should be mentioned that χ may only be determined in the temperature regime well above the T_g of the PS block and in the disordered state. This is where the inverse peak intensity varied linearly with the inverse temperature. It is obvious in Figure 4a that χ shows different temperature dependencies for various compositions. χ depends on both temperature and composition, for the enthalpic and entropic parts of χ as shown in Figure 4b,c. A minimum of χ can be observed near the symmetric composition which was also found for other block copolymer systems.[27] This may be due to the fact that χ is an effective interaction parameter based on mean-field theory. In the present case it is very small, and other contributions not considered in the theory might gain comparable importance. The mean-field theory, which is based on equal Kuhn segment length and monomer volumes of the corresponding homopolymers, cannot explain a composi-

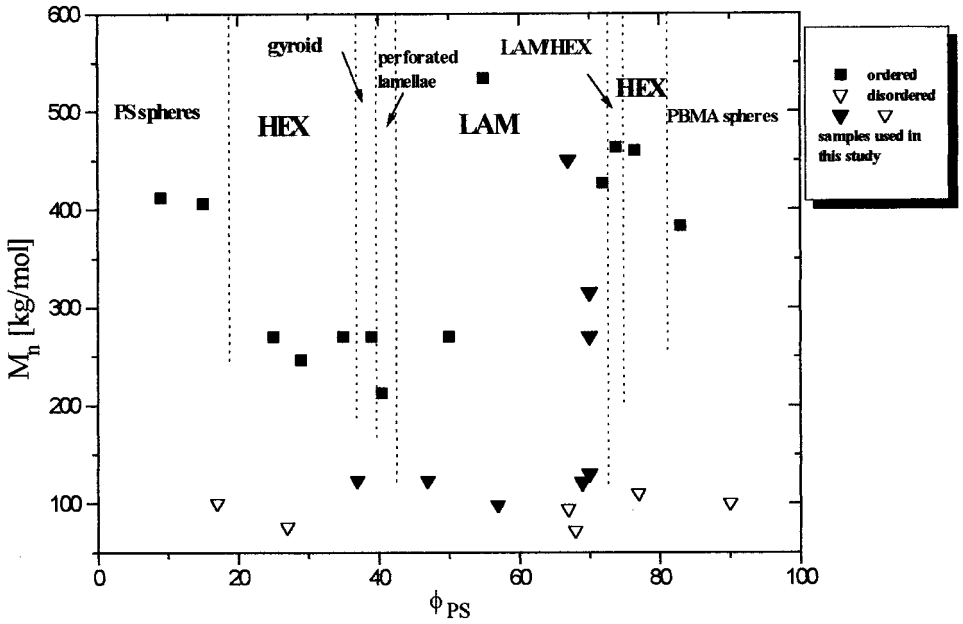

Figure 2. Morphologies for PS-*b*-PBMA diblock copolymers used in this study and discussed in refs 22, 23, and 25.

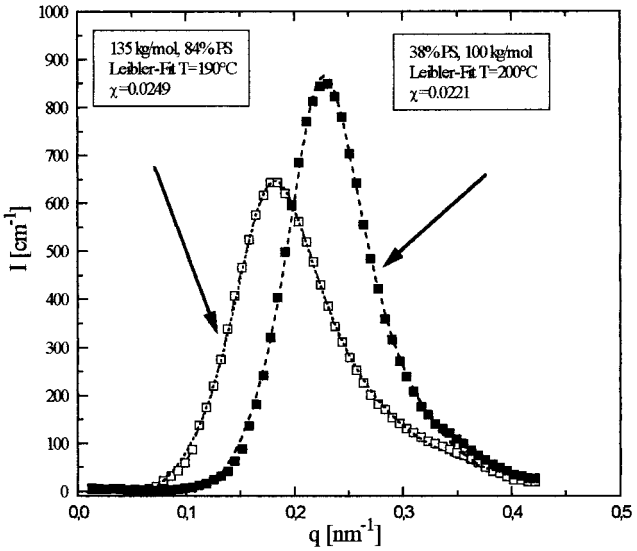

Figure 3. Representative Leibler fits to scattering curves of asymmetric dPS-*b*-PBMA diblock copolymers in the disordered state.

tion dependence of the χ parameter. However, the segment length and monomer volume of the corresponding components in PS-*b*-PBMA are different. For polymer blends, the composition dependence of χ is given by the theory of Freed and Dudowitz.[28] Furthermore, a dependence of χ on molecular weight is also included in the lattice cluster model of Freed and Dudowitz[28] for polymer blends. For PS-*b*-PBMA diblock copolymers we also found an increasing χ with increasing molecular weight[25] which is in agreement with observations in other systems.[29] For PS-*b*-PBMA diblock copolymers, the interaction parameter depends on composition as well as on molecular weight, and the phase behavior appears to be quite complex. Therefore, the $\chi N-\varphi$ phase diagram cannot be discussed in the present study, and further investigations are necessary to calculate $(\chi N)_{crit}$ values for different compositions.

However, it is possible to discuss the correlation between phase behavior and deformation mechanims of PS-*b*-PBMA diblock copolymers based on the χN values at different compositions.

2. Correlation between Phase Behavior and Deformation Mechanisms. 2.1. Influence of Composition. To investigate the influence of composition on deformation behavior of PS-*b*-PBMA diblock copolymers, samples with an overall molecular weight of about 100 kg/mol and different polystyrene contents are used (sample series 1 in Table 2). Our results will be focused on the change of deformation mechanism (crazing, cavitation) and micromechanical structure.

For block copolymers with PS contents smaller than 37%, no local deformation zones or crazes can be found by HVEM. For samples with $\varphi_{PS} = 0.37$, a transition from homogeneous deformation to local deformation zones can be found. Also at higher PS contents, local deformation zones exist, indicating a change of deformation mechanism at this composition. The disordered state of block copolymers at small PS contents associated with a homogeneous deformation is also found for PBMA.

If we compare the deformation structure in PS in Figure 5 with sample P57 in Figure 6, it is obvious that the deformation structure of sample P57 differs from that of PS. Clearly visible are the highly deformed fibrils in the deformation zones of sample P57. The PS fibrils appear to be dark because of their larger thickness compared to that of PBMA. It is easily seen that the craze fibrils are much thicker than those observed in PS; this is mainly arising from the lamellar structure of the block copolymer P57. The morphology is not shown in Figure 6 because the sections used for HVEM investigations reveal a thickness on the order of 500 nm, which is much larger than the thickness of the lamellae (long period 40 nm). It was shown previously[12] that the craze structures in block copolymers arise from their microphase-separated morphology. However, many craze fibrils are larger than the thickness of the lamellae due to the coalescence of many smaller craze fibrils. The result that the deformation structure in sample P57 differs from that of PS is consistent with observation by Argon and co-workers[9-11] and our previous results[12] that deformation in block copolymers occurs via cavitation. It is visible in Figure 6 that both blocks, PS and

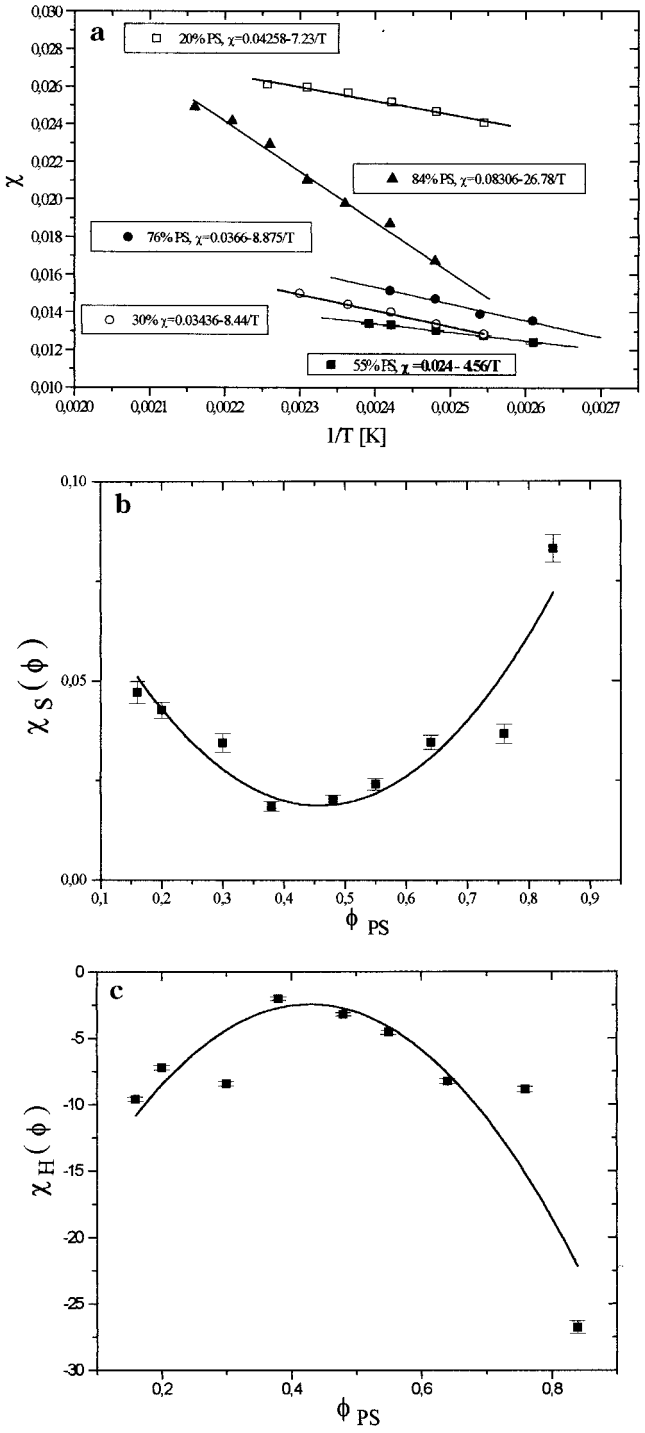

Figure 4. (a) Temperature dependencies of χ for PS-*b*-PBMA diblock copolymers with different compositions ($\chi = \chi_S + \chi_H/T$ where χ_S is the entropic and χ_H is enthalpic contribution to χ). The errors of χ are small as representatively shown in the case of a sample with 55% dPS. (b) Compositional dependence for entropic part (χ_S) and (c) enthalpic part (χ_H) of interaction parameter χ for PS-*b*-PBMA diblock copolymers at $T = 150$ °C.

PBMA, are highly deformed due to the cavitation mechanism. This means that the craze growth in sample P57 occurs via cavitation. The PBMA lamellae can be easily deformed due to their low modulus and is followed by a large plastic deformation of the PS phase due to the high stress concentration at the PS lamellae. This is clearly consistent with the two-step cavitation mechanism reported by Argon and co-workers[9−11] for PS-*b*-PB diblock copolymers.

Table 2. Molecular Weight (M_n), Volume Fraction (Φ_{PS}), χN Values at 120 °C (Based on Composition Dependent χ Parameter), and Morphology (TEM) for PS-*b*-PBMA Diblock Copolymers Used in This Study

sample	$10^{-3}M_n$[a] copolymer	φ_{PS} block[b]	morphology (TEM)	χN
series 1				
P17	100.8	0.17	disordered	17.46
P27	75.9	0.27	disordered	10.38
P37	123.0	0.37	ordered	14.23
P47	123.0	0.47	lamellae	11.92
P57	98.4	0.57	lamellae	10.60
P67	94.0	0.67	disordered	11.55
P77	110.8	0.77	disordered	14.02
P90	100.1	0.9	disordered	21.55
series 2				
SBM72	71.8	0.68	disordered	8.84
SBM94	94.0	0.67	disordered	11.55
SBM120	121.2	0.69	lamellae	14.94
SBM130	130.0	0.70	lamellae	16.10
SBM270	270.0	0.70	lamellae	33.45
SBM315	315.0	0.70	lamellae	39.03
SBM450	450.0	0.67	lamellae	55.28

[a] Total molecular weight and polydispersity determined by size exclusion chromatography (SEC); values are based on the PS standards. The polydispersity is less than 1.1 for all samples. [b] Volume fraction of PS determined by ^{1}H NMR.

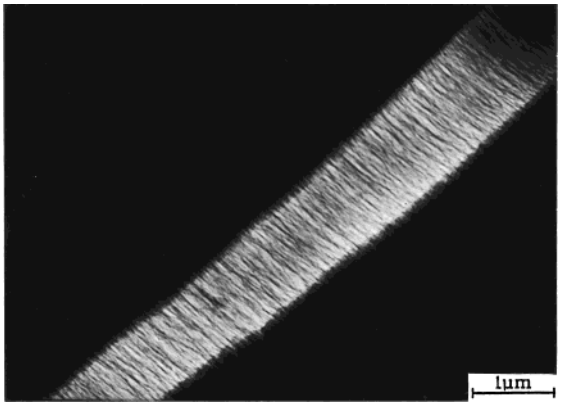

Figure 5. HVEM micrograph of craze structure in PS with $M_n = 313$ kg/mol; strain direction is parallel to craze fibril direction.

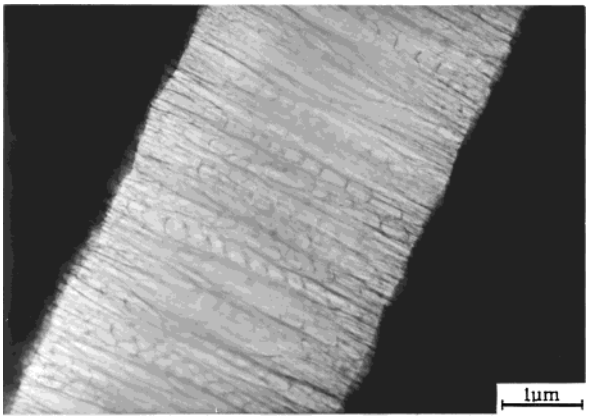

Figure 6. HVEM micrograph of craze structure of sample P57 ($\Phi_{PS} = 0.57$, $M_n = 98.4$ kg/mol) with lamellar morphology; strain direction is parallel to craze fibril direction.

It is shown in Figure 6 that many of the thicker craze fibrils span over the entire craze. Furthermore, many cross-tie fibrils can be observed in this block copolymer, stabilizing the craze structure. The thickness of the craze fibrils seems to be quite large at values up to 50 nm. To confirm that these thicker craze fibrils arise from

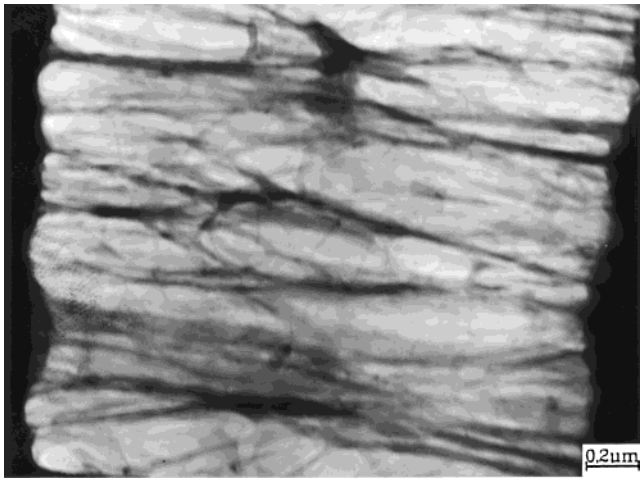

Figure 7. Higher magnification of a craze structure of a lamellar PS-*b*-PBMA diblock copolymer P57 ($\Phi_{PS} = 0.57$, $M_n = 98.4$ kg/mol); strain direction is parallel to craze fibril direction.

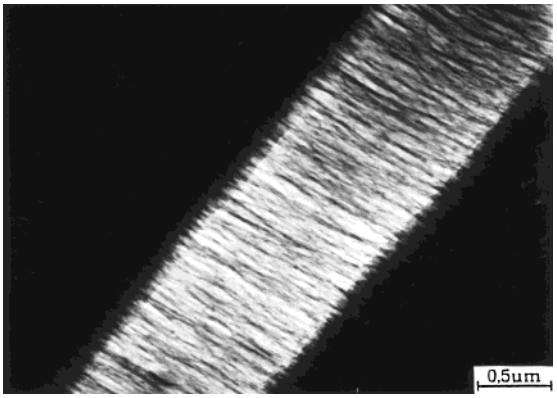

Figure 8. HVEM micrograph of craze structure of a disordered PS-*b*-PBMA diblock copolymer P67 ($\Phi_{PS} = 0.67$, $M_n = 94$ kg/mol); strain direction is parallel to craze fibril direction.

a coalescence of thinner ones as well as from a overlap of fibrils, a higher magnification of craze structure in sample P57 is shown in Figure 7. Many fibrils with different orientations are visible in Figure 7, resulting in a network-like craze structure. Furthermore, many of the thinner craze fibrils with greater variety of orientations exist in the craze. This craze structure indicates that the sample is deformed via cavitation of lamellar morphology with small grains at different orientations. The poor long-range order of this sample is due to their high miscibility.

Figure 8 shows a representative deformation structure in a disordered block copolymer (sample P67). The deformation structure changes significantly when compared to that of block copolymers with lamellar structures. As shown in Table 3, the diameter of the craze fibrils is about 10 nm for samples with 67−90% PS. This value is close to that of PS as observed by other authors[30,31] and shown in Figure 5. Furthermore, the distance between the craze fibrils of about 10−50 nm is comparable with PS. The pattern of deformation structure does not change during in-situ tests starting from an initial undeformed state. This means that the mixed phase in sample P67 is not deformed by the two-step mechanism of cavitation but shows a crazing mechanism. The absence of a microphase-separated morphology avoids the deformation of the PBMA phase as a first step of the cavitation. Therefore, the deformation of the mixed phase occurs via crazing.

Table 3. Deformation Mechanisms, Diameter of Craze Fibrils, and Craze Lengths in PS-*b*-PBMA Diblock Copolymers Depending on Volume Fraction of PS (Sample Series 1 in Table 2)

sample series 1 in Table 2	deformation mechanism	diameter of craze fibrils [nm]	craze length [μm]
PS	crazing	2.5−10	10−50
P90	crazing	max 10	max 100
P77	crazing	max 10	max 150
P67	crazing	max 10	max 150
P57	cavitation	max 50	max 500
P47	cavitation	max 50	max 300
P37	homogeneous/ cavitation	20−50	20−50
P17	homogeneous		
PBMA	homogeneous		

From these results, we can conclude that a transition from cavitation to crazing occurs at 67% PS content, and the reason for the observed transition from cavitation to crazing mechanism is the disordered state at of this sample.

Figure 9 shows deformation zones in diblock copolymers with different compositions observed at low magnification. Most of the crazes reveal a thickness of about 1−2 μm, with some crazes showing a larger thickness of up to 4 μm. With increasing PS content, the craze length increases from 20 to 50 μm for sample P37 up to about 500 μm for sample P57. At 57% PS, a maximum of craze length can be observed (Figure 10). For block copolymers with higher PS contents the craze length decreases and shows almost the value of homopolystyrene. It was found that crazes in PS are large in number, but short, and randomly distributed.[32,33] Comparing this with block copolymers having 47 and 57% PS, it is found that crazes in PS-*b*-PBMA are fewer but much longer than observed in PS. A similar result was found by Koltisko[32] for SBS triblock copolymers and by Weidisch and co-workers[12] for PS-*b*-PBMA with $M_n > 200$ kg/mol. It was already discussed that block copolymers in the composition range of $0.37 < \varphi_{PS} < 0.57$ are ordered and samples with other compositions are disordered. Therefore, the craze length shows a maximum for block copolymers with lamellar structures.

Our investigations have shown that the transition from cavitation to crazing at 67% PS is attributed to the order−disorder transition with increasing PS content. While ordered block copolymers show a cavitation mechanism, disordered diblock copolymers with high PS contents reveal a crazing mechanism. This result allowed us to correlate the deformation behavior with tensile properties shown in Figure 11. The values of craze initation stress, σ_c, in Figure 11 are obtained from stress−strain curves where a deviation from their linear slope may be found.[12] Therefore, the values of σ_c are correlated with tensile properties and are shown to have a maximum of σ_c for block copolymers at 57% PS. For block copolymers with $\varphi_{PS} > 0.57$, the craze initiation stess decreases due to the disordered state of these samples. The maximum of σ_c at 57% PS corresponds to a lamellar morphology[34] which provides reasons for the maximum in tensile stength at this composition, because the plastic deformation occurs at a higher level of stress. Samples with PS contents higher than 57% are brittle, and their tensile strength is smaller than that of PS.[34]

2.2. Influence of Molecular Weight. To investigate the influence of χN on deformation behavior, a second

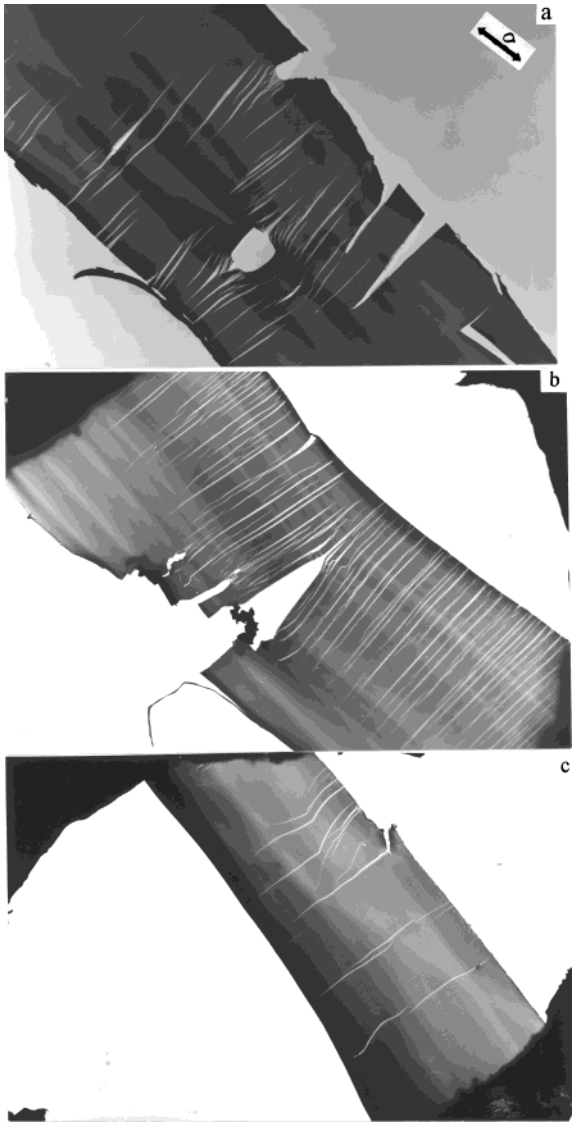

Figure 9. Lower magnifications of crazes in PS-*b*-PBMA diblock copolymers: (a) P47 ($\Phi_{PS} = 0.47$, $M_n = 123$ kg/mol), (b) P57 ($\Phi_{PS} = 0.57$, $M_n = 98.4$ kg/mol), and (c) P77 ($\Phi_{PS} = 0.77$, $M_n = 100.1$ kg/mol); strain direction is perpendicular to craze growth.

series of PS-*b*-PBMA diblock copolymers with an approximately composition of 65−70% PS and different molecular weights (71−450 kg/mol) are investigated (sample series 2 in Table 2).

Figure 12 shows a craze structure within sample SBM71 with 71 kg/mol. The craze structure is almost the same as PS, which demonstrates that the deformation in this block copolymer occurs via crazing. Using the Flory−Huggins interaction parameter, χ, it is possible to correlate the phase behavior with deformation mechanism. For sample SBM71, χN is 8.8, indicating that this sample is disordered. The order−disorder transition occurs only at $\chi N = 14.9$ for a asymmetric diblock copolymer with 70% of one component according to Leibler theory,[35] which was also found by TEM and DMA.[34] This explains the crazing mechanism shown by this block copolymer, confirming our previous discussion of deformation behavior of PS-*b*-PBMA diblock copolymers in the disordered state. For sample SBM71 a crazing mechanism can be observed, while for sample SBM130 (130 kg/mol) a transition from crazing to cavitation mechanism occurs. This is shown in Figures

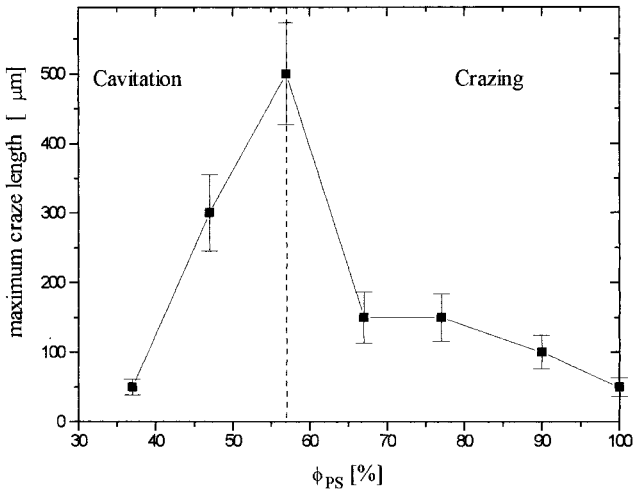

Figure 10. Dependence of craze length on composition for PS-*b*-PBMA diblock copolymers in Table 2 (sample series 1) after applying a 2% strain.

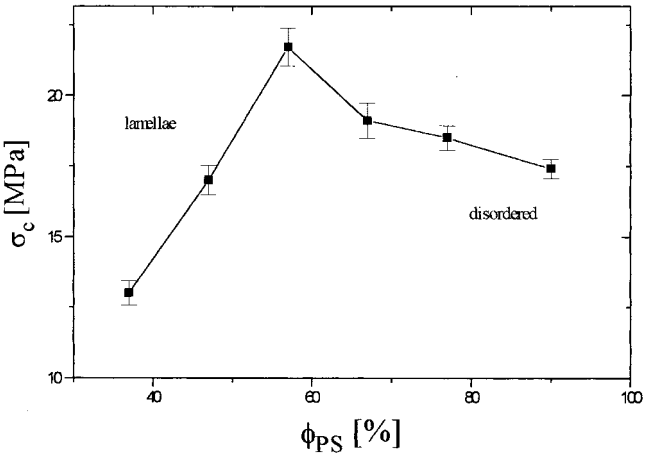

Figure 11. Dependence of craze initiation stress, σ_c, on volume fraction of PS for PS-*b*-PBMA diblock copolymers (sample series 2 in Table 1).

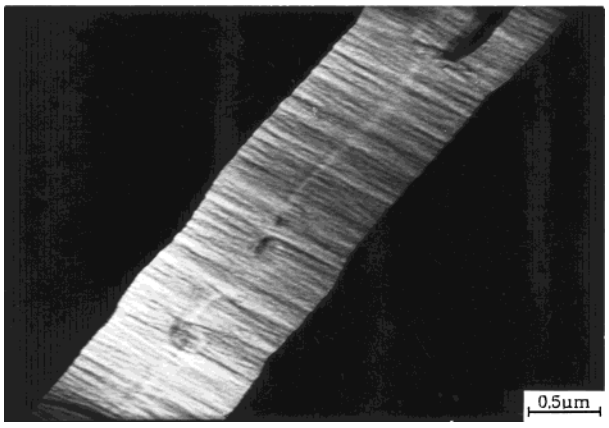

Figure 12. HVEM micrograph of craze structure of a PS-*b*-PBMA diblock copolymer at $\chi N = 8.8$ (SBM72, $\Phi_{PS} = 0.68$, $M_n = 71.8$ kg/mol, disordered); strain direction is parallel to craze fibril direction.

12 and 13 which confirm our previous results. The transition from a disordered to an ordered state by increasing molecular weight is clearly associated with the change of deformation mechanism from crazing to cavitation as χN is increased from 8.8 to 16.1. With a further increase of molecular weight, no change in the deformation mechanism occurs such that a cavitation

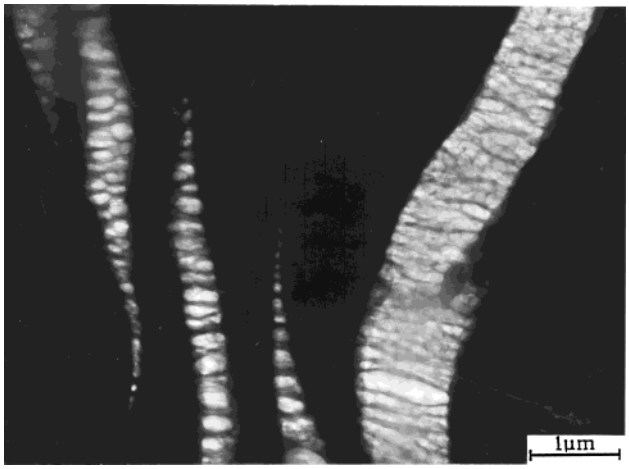

Figure 13. HVEM micrograph of craze structure of a weakly segregated PS-*b*-PBMA diblock copolymer at $\chi N = 16.1$ (SBM130, $\Phi_{PS} = 0.70$, $M_n = 130$ kg/mol, lamellae); strain direction is parallel to craze fibril direction. A transition from crazing to cavitation mechanism can be observed.

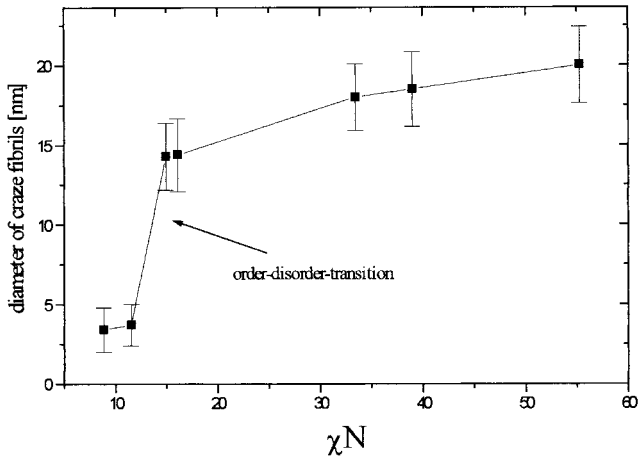

Figure 14. Dependence of diameter of craze fibrils on strength of segregation χN for PS-*b*-PBMA diblock copolymers with approximately 70% PS (sample series 2 in Table 2).

mechanism is observed for all block copolymers in the ordered state.

Figure 14 shows the correlation between craze structure and strength of segregation, χN, which gives us the possibility to correlate the deformation structure in block copolymers with phase behavior. It is obvious from Figure 14 that the diameter of the craze fibrils changes significantly at the phase transition. Both deformation mechanism and craze microstructure are strongly influenced by phase behavior. It is interesting to note that the shear modulus as well as the scattering intensity shows a strong change at the phase transition,[36−38] but Figure 14 also characterizes the deformation structure of block copolymers. This confirms that the phase behavior of block copolymers has a pronounced influence on deformation behavior which explains the reported correlation between phase behavior and tensile properties.[21,34] An increase in the thickness of craze fibrils is also associated with improved tensile properties because thicker fibrils can sustain a higher stress level. It is obvious in Figure 14 that the diameter of craze fibrils shows a further increase in diameter as χN is raised. It was shown by various authors[39,40] that between the weak (WSL) and strong segregation limits (SSL) an intermediate segregation regime (ISR) exists between

Figure 15. HVEM micrograph of deformation zones of an intermediately segregated PS-*b*-PBMA diblock copolymer at $\chi N = 39$ (SBM315, $\Phi_{PS} = 0.70$, $M_n = 315$ kg/mol, lamellae). The craze propagation is influenced by morphology and does not occur perpendicular to the external stress direction in all cases.

$12.5 < \chi N < 95$ (crossover between ISR and SSL at $\chi N \approx 50$). In the ISR the chains are stretched due to the coarsening of the density profile as χN is increased from the WSL. Within the ISR the interface is broadened, and the junction points are not completly localized within the interfacial region. While samples SBM71 ($\chi N = 8.84$) and SBM94 ($\chi N = 11.55$) are disordered and sample SBM120 ($\chi N = 14.94$) is weakly segregated, block copolymers with higher χN (Table 2) are intermediately segregated. A further change of craze structure in the ordered state can be attributed to the increase of long period with increasing molecular weight. It was shown from bulk samples that a significant increase of strain at break can be observed as χN increases.[34] At the phase transition, a change of fracture mode from brittle to tough was observed corresponding to the transition from crazing to cavitation.[34] The tensile strength and strain at break achieve their maximum in the ISR.[23,34] The strain at break increases from 12% at $\chi N = 16.1$ (sample SBM130) up to about 30% at $\chi N = 33.45$ (sample SBM270) in the ISR. For an intermediately segregated diblock copolymer with $\chi N = 39$ (SBM315), large deformation zones can be observed (Figure 15). This was also found for a sample with $\chi N = 55.3$ as reported in our previous study.[12] Crazes with a thickness up to 5−6 μm arise from a coalescence of thin deformation zones not observed in weakly segregated block copolymers with lower molecular weights. Furthermore, mechanisms such as termination of crazes and diversion of crazes are also observed in intermediately segregated block copolymers. It is obvious in Figure 15 that the crazes do not propagate perpendicular to external stress field in all cases. This arises from the influence of morphology on craze propagation as discussed in detail.[12] It was shown in one of our previous papers[34] that the long-range order significantly increases as χN increases from 16.1 (sample SBM130) to 33.45 (sample SBM270). The grain size increases with increasing incompatibility from about 500 nm up to 3−5 μm. Therefore, mechanisms such as diversion and termination of crazes are only effective if the grain size is large enough. These deformation mechanisms are associated with the formation of stable crazes as shown in Figure 15. A higher magnification of this process is shown in Figure 16 where stacks of lamellae oriented perpendicular to external stress field are highly de-

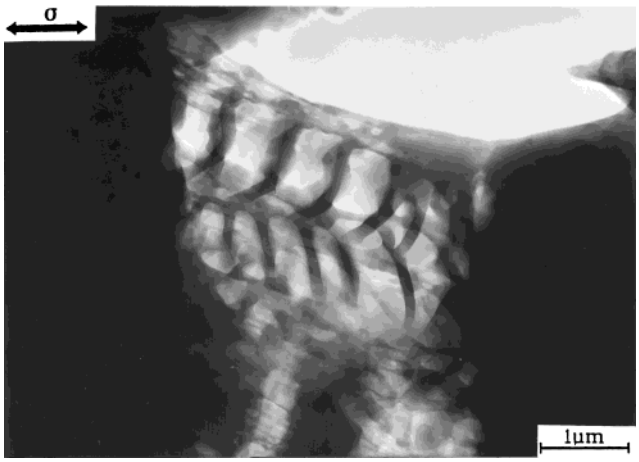

Figure 16. Higher magnification of a deformation structure of a lamellar PS-*b*-PBMA diblock copolymer (SBM315, $\Phi_{PS} = 0.70$, $M_n = 315$ kg/mol).

formed. The shape of this deformation zones is similar to a "breastbone", indicating the formation of a stable deformation zone which can sustain a high level of stress. Formation of these deformation zones is accompanied by a large plastic deformation of the PS lamellae. The PBMA lamellae cavitate, followed by a large deformation of stacks of PS and PBMA lamellae in the stress direction by a drawing process. This is indicated by the large distances between the lamellae arising from a plastic deformation of more than 400%. This drawing process can be discussed in addition to the already reported mechanisms of diversion of crazes and rotation of lamellae.[12] These processes explain the sharp increase of strain at break for block copolymers in the ISR. The high tensile strength of this PS-*b*-PBMA diblock copolymers can be explained by their broadened interface width and increased craze initiation stress.[12,21]

The phase behavior has a pronounced influence on deformation behavior as well as on deformation structure. While disordered PS-*b*-PBMA diblock copolymers at high PS contents show a crazing mechanism, a change to cavitation mechanism occurs at the order−disorder transition. Both the deformation mechanism and deformation structure strongly change at the phase transition. Disordered block copolymers show the deformation mechanism of the corresponding homopolymers which clearly shows that the microphase-separated morphology of block copolymers is the reason for the observation of a cavitation mechanism. With increasing incompatibility mechanisms of termination and diversion of crazes, rotation of lamellae[12,41] and drawing of stacks of lamellae (Figure 16) can be observed which are associated with a growth of large deformation zones. While the phase transition to ordered state is the reason for the change of deformation mechanism to cavitation, the discussed deformation mechanisms for intermediately segregated PS-*b*-PBMA diblock copolymers can be attributed to the increase of long-range order with increasing incompatibility. The increasing incompatibility is associated with a change of morphology which is responsible for a change in the local stress field and stress concentrations in the domains. Stress concentrations lead to plastic deformations and may enhance the toughness of the block copolymers. This holds true if the craze fibrils can sustain a high level of stress while yielding. The broadened interface in intermediately segregated block copolymers is associated with an increase of craze initiation stress which is responsible for an improvement of tensile properties.[21,23]

Conclusions

It was possible to correlate the phase behavior of PS-*b*-PBMA diblock copolymers with deformation mechanism and deformation structure. This correlation is based on the investigation of phase behavior which depends on molecular weight and composition. It was shown that the Flory−Huggins parameter, χ, depends not only on temperature but also on composition.

Our investigations have shown that the phase behavior of block copolymers has a pronounced influence on deformation mechanisms as well as deformation structure. The deformation structure of block copolymers arises from their microphase-separated morphology, and the order−disorder transition is associated with a change from cavitation to crazing. Both studies, depending on composition and on molecular weight, confirm that disordered block copolymers show the same deformation mechanism as the corresponding homopolymers. The investigation of deformation mechanisms and craze structure may be used to understand the influence of phase behavior on tensile properties. The maximum tensile strength corresponds to a maximum in craze initation stress and craze length.

Clearly the deformation behavior has a dependence on the strength of segregation, χN. An interesting feature is that, in addition to shear modulus and scattering intensity, the craze microstructure undergoes a sharp transition as shown in Figure 14.

We have also demonstrated how the phase behavior influences the deformation behavior and the craze structure of block copolymers. Within the WSL, a cavitation mechanism is observed, while the ISR is associated with additional deformation mechanisms such as diversion and termination of crazes, in addition to rotation and drawing of lamellae.

The correlation between phase behavior and deformation mechanisms indicates the existence of a unified scheme for deformation behavior in diblock copolymers depending on strength of segregation. Investigation of other block copolymer systems should confirm this correlation. While a crazing mechanism may found in disordered block copolymers, the deformation occurs via cavitation in the WSL. In the ISR, mechanisms of diversion and termination of crazes are both observed in addition. On the basis of these observations, it then becomes possible to predict the deformation behavior of a block copolymer system from the strength of segregation (χN) and morphology. This correlation, however, should be proved by using different block copolymer systems, since it is only discussed for PS-*b*-PBMA diblock copolymers in the present study.

Acknowledgment. R. Weidisch acknowledges financial support from Deutsche Forschungsgemeinschaft (DFG). We also acknowledge the help of Dr. P. Staron during the SANS measurements at GKSS Geesthacht (Germany). This work was supported in part by the Landesprojekt Sachsen-Anhalt "Neue Funktionswerkstoffe auf der Grundlage schwach entmischter Blockcopolymere".

References and Notes

(1) Thomas, E. L.; Alward, D. B.; Kinning, D. J.; Martin, D. C.; Handlin, D. L.; Fetters, L. J. *Macromolecules* **1987**, *20*, 1651.

(2) Winey, K. I.; Gobran, D. A.; Xu, Z.; Fetters, L. J.; Thomas, E. L. *Macromolecules* **1994**, *27*, 2392.
(3) Spontak, R. J.; Smith, S. D.; Ashraf, A. *Macromolecules* **1993**, *34*, 2233.
(4) Hamley, I. W.; Koppi, K. A.; Rosedale, J. H.; Bates, F. S.; Almdal, K.; Mortensen, K. *Macromolecules* **1993**, *26*, 5959.
(5) Hadjuk, D. A.; Harper, P. E.; Gruner, S. M.; Honeker, C. C.; Kim, G.; Thomas, E. L.; Fetters, L. J. *Macromolecules* **1994**, *27*, 4063.
(6) Förster, S.; Khanpur, A. K.; Zhao, J.; Bates, F. S.; Hamley, I. W.; Ryan, A. J.; Bras, W. *Macromolecules* **1994**, *27*, 6922.
(7) *Thermoplastic Elastomers*; Legge, N. R., Holden, G., Schroeder, H. E., Quirk, R. P., Eds.; Hanser: Muinch, 1996.
(8) Yamaoka, I. *Polymer* **1998**, *39*, 1765.
(9) Schwier, C. E.; Argon, A. S.; Cohen, R. E. *Polymer* **1985**, *26*, 1985.
(10) Argon, A. S.; Cohen, R. E. In *Crazing in Polymers*; Kausch, H. H., Ed.; Springer Verlag: Berlin, 1983; Vol. 1.
(11) Argon, A. S.; Cohen, R. E. In *Crazing in Polymers*; Kausch, H. H., Ed.; Springer Verlag: Berlin, 1990; Vol. 2.
(12) Weidisch, R.; Ensslen, M.; Michler, G. H.; Fischer, H. *Macromolecules* **1999**, *32*, 5375.
(13) Polis, D. L.; Winey, K. I. *Macromolecules* **1998**, *31*, 3617.
(14) Segula, R.; Prud'homme, J. *Macromolecules* **1985**, *18*, 1295.
(15) Odell, J. A.; Keller, A. *Polym. Eng. Sci.* **1977**, *17*, 544.
(16) Pakula, T.; Saijo, K.; Kawai, H.; Hashimoto, T. *Macromolecules* **1985**, *18*, 1295.
(17) Sakamoto, J.; Sakurai,; Doi, K.; Nomura, S. *Macromolecules* **1993**, *26*, 3351.
(18) Dair, B. J.; Honeker, C. C.; Alward, D. B.; Avgeropoulos, A.; Hadjichristidis, N.; Fetter, L. J.; Capel, M.; Thomas, E. L. *Macromolecules* **1999**, *32*, 8145.
(19) Russell, T. P.; Karis, T. E.; Gallot, Y.; Mayes, A. M. *Nature* **1994**, *368*, 729.
(20) Ruzette, A.; Banerjee, P.; Mayes, A. M.; Pollard, M.; Russell, T. P.; Jerome, R.; Slawecki, T.; Hjelm, R.; Thiyagarajan, P. *Macromolecules* **1998**, *31*, 8509.
(21) Weidisch, R.; Stamm, M.; Schubert, D. W.; Arnold, M.; Budde, H.; Höring, S. *Macromolecules* **1999**, *32*, 3405.
(22) Weidisch, R.; Michler, G. H.; Fischer, H.; Hofmann, S.; Arnold, M.; Stamm, M. *Polymer* **1999**, *40*, 1191.
(23) Weidisch, R.; Stamm, M.; Michler, G. H.; Fischer, H.; Jerome, R. *Macromolecules* **1999**, *32*, 742.
(24) Arnold, M.; Hofmann, S.; Weidisch, R.; Neubauer, A.; Poser, S.; Michler, G. H. *Macromol. Chem. Phys.* **1998**, *199*, 31.
(25) Fischer, H.; Weidisch, R.; Stamm, M.; Budde, H.; Höring, S. *Colloid Polym. Sci.*, in press.
(26) Russell, T. P.; Hjelm, R. P.; Seeger, P. A. *Macromolecules* **1990**, *23*, 890.
(27) Bates, F. S.; Muthukumar, M.; Wignall, G. D.; Fetters, L. J. *J. Chem. Phys.* **1988**, *89*, 535.
(28) Dudowitz, J.; Freed, K. F. *Macromolecules* **1993**, *26*, 213.
(29) Schweizer, K. S.; Curro, J. G. *Adv. Polym. Sci.* **1994**, *116*, 319.
(30) Michler, G. H. *Ultramicroscopy* **1984**, *15*, 81.
(31) Beahan, P.; Bevis, M.; Hull, D. *J. Mater. Sci.* **1973**, *8*, 162.
(32) Koltisko, B.; Hiltner, A.; Baer, E. *J. Polym. Sci., Polym. Phys.* **1986**, *24*, 2167.
(33) Donald, A. M.; Chan, T.; Kramer, E. J. *J. Mater. Sci.* **1981**, *16*, 669.
(34) Weidisch, R.; Michler, G. H.; Arnold, M. *Polymer* **2000**, *41*, 2231.
(35) Leibler, L. *Macromolecules* **1980**, *13*, 1302.
(36) Stühn, B.; Mutter, R.; Albrecht, T. *Europhys. Lett.* **1992**, *18*, 427.
(37) Rosedale, J. H.; Bates, F. S.; Almdale, K.; Mortensen, K.; Wignall, D. *Macromolecules* **1995**, *28*, 1429.
(38) Hamley, I. W. *The Physics of Block Copolymers;* Oxford University Press: New York, 1998.
(39) Matsen, M. W.; Bates, F. *Macromolecules* **1996**, *29*, 1091.
(40) Melenkevitz, J.; Muthukumar, M. *Macromolecules* **1991**, *24*, 4199.
(41) Polis, D. L.; Smith, S. D.; Terril, N. J.; Ryan, A. J.; Morse, D. C.; Winey, K. I. *Macromolecules* **1999**, *32*, 4668.

MA991660V